HANDBOOK OF CHEMICAL AND BIOCHEMICAL TECHNOLOGIES

CHAPTER 6: THE ROLE OF CHEMICAL SYNTHESIS IN THE SUSTAINABILITY OF ORGANIC DYE-SENSITIZED SOLAR CELLS

1. Introduction

The production of an efficient and novel π-extended D-A-π-A natural sensitizer (G3, η = 8.64%) intended for solar cells that are dye-sensitized has been achieved by the application of the green chemistry pillars. It aims at overriding conventional routes that involved organo-metallic intermediates with novel synthetic strategies for reduction I the production of waste material as well as reducing dye production costs. Research has shown that complex target sensitizer can be exclusively obtained through direct arylation reactions. Comparison between green metrics with that of a conventional synthetic pathway indicates that the novel approach, without a doubt, has a lower impact on the environment regarding generated wastes and chemical procedures. This, in turn, stresses on the significance of the synergy among the synthetic plan and the molecular design in the framework of ecological friendly routes to support the sustainable development of third-generation photo-voltaic. Moreover, an investigation was also carried out to inspect the stability of the G3-based photovoltaic devices in aging tests on devices having large area which demonstrated the excellent potential of the planned structure for all practical applications that involve organic dye interfaces/ inorganic semiconductor (Ooyama et al., 2011; Ooyama & Harim, 2012; 2013).

Constant research has been ongoing to find the potential alternative to the commercially available photovoltaic technologies. One major attraction for this purpose is dye-sensitized solar cells (DSSCs) who have been a focus of attention due to various aspects such as ease of fabrication, their high efficiencies of conversion from light-to-energy, their distinctive peculiarity in terms of coloration and transparency, which enables the design of proficient, vibrant smart panels and devices also amenable to building integration (Yen et al., 2012; Liang & Chen, 2013; Zhang et al., 2013). The typical configuration of a DSSC is composed of a counter-electrode, a photo-anode (normally a duly dye-sensitized semiconducting film made of mesoporous Titania material) and an electrolyte that contain a redox couple (O'regan & Grätzel, 1991; Mishra et al., 2009; Zeng et al., 2010). A major portion of the research on DSSC has its focus on the dye, which is responsible for the harvesting of photons as well as assisting the injection of an electron into the Titania conduction band (Ogura et al., 2009; Yum et al., 2012; Fan et al., 2011). Nevertheless, the selection of the sensitizer greatly influences not just the efficiency of the device but also most of the environmental factors and price associated with the production of technology (Zardetto et al., 2013; Fakharuddin et al., 2014; Matteocci et al., 2016). As a result, with particular reference to the sensitizer, even though it is permissible that fundamental research on DSSCs should focus to struggle for the accomplishment of higher and higher efficiencies, part of

this research must also be directed towards minimizing the environmental effect that is related to the production of DSSCs.
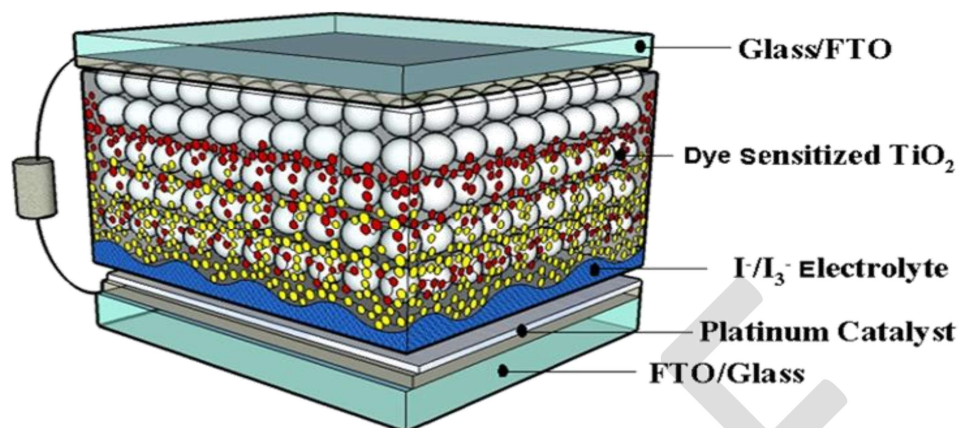

Fig. 52. Typical configuration of a Dye Sensitized Solar Cell (DSSC)

[Source: https://schanze.chem.ufl.edu/research/dye-sensitized-solar-cells/]

Sensitizers that are fully organic have shown great potential in both amenabilities to optimization and design flexibility regarding performances of devices (Hagfeldt et al., 2010; Yella et al., 2011; Mishra et al., 2009). From the environmental point of view, application of organic dyes calls off the requirement of restoring to rarely occurring heavy metals such as ruthenium or exceptionally toxic ones like lead (a constituting element of solar cells based on perovskite material and presently currently in the "spotlight" due to their high efficiency) for the environmental impacts that involve both production as well as post-life disposal (Gao et al., 2014; Green et al., 2014; Sum & Mathews, 2014).

Among various proposed molecular architectures, synthesis of an extensive number of organic dyes has been carried out as per the D-π-A concept, by putting in fitting conjugation an electron-withdrawing group (A) and an electron-donating group (D) having the ability to bind to the Titania through an appropriate π-spacer (π), the former being the primary focus of current structural tailoring intended for expansion of the light-harvesting range (Wu et al., 2012; Yen et al., 2012; Wu & Zhu, 2013). From the point of view of synthetic chemistry, the downside of the D-π-A concept is associated with the asymmetric structure of the sensitizers, which inevitably leads to a high number of synthetic steps needed for obtaining the target molecule (He et al., 2014; Xiao et al., 2014; Xing et al., 2017).

Simultaneously, it is important to recognize that the main concern for the market breakthrough of DSSC will be to bridge the gap that exists between research of the fundamental materials and their scalability. In fact, customary laboratory practice puts a higher strain on the environment; furthermore, it is not always possible to transfer it to an industrial scale. The assurance of environmental sustainability is important since the key challenges in environmental science are not merely associated with exploitation

of renewable energy sources but also for assessment, monitoring and minimization of the effect related to the chemistry of materials behind a green technology (Burke & Lipomi, 2013 Osedach et al., 2013; Po et al., 2014). For that reason, novel methods followed for organic synthesis of highly capable organic sensitizers that help maximizing sustainability (mainly in terms of amount of waste) are incredibly desirable, being potentially open to scalability without causing any severe impact on the environment (Zhang et al., 2012; 2013; He et al., 2014).

In this regard, synthetic protocols that are based on the activation of C−H bond for constructing a π-conjugated scaffold can be considered the superior tool for reducing the number of synthetic steps, since they allow evading the preparation of organo-metallic intermediates that are required for the conventional cross-coupling methods (Schipper & Fagnou, 2011; Berrouard et al., 2012; Mercier & Leclerc, 2013). The rarity of examples that employ functioning of C−H bond for synthesizing organic sensitizers may be linked to the fact that few restrictions of the existing C−H activation protocols (such as the low selectivity in the presence of two or more active bonds) appear to form an undefeatable obstacle when applied to the assemblage of the complicated asymmetric structures of D-π-A organic sensitizers (Kang et al., 2014; Chai et al., 2015; Joly et al., 2015).

The main idea underlying this work is to exhibit that the roadmap directed towards highly capable dyes can be escorted with an appropriate plan of cleaner synthetic methodologies (Feng et al., 2013; Qian et al., 2015). This work focusses on the application of the principles of green biotechnology about the production of reduced waste material and the utilization of hazardous reactants (Double, 2014; Jiang et al., 2014; Li et al., 2014; Echeverry et al., 2015). On these grounds, in continuation with our studies on the function of a π-bridge extension in benzothiadiazole-based D-A-π-A sensitizers, a novel dye has been conceived (known as G3, Fig.53) by application of the simplest obtainable aromatic units (benzothiadiazole, thiophene, benzene) to call for an optimum DSSC work cycle (Grisorio et al., 2014; Liu et al., 2014; Roiati et al., 2015).
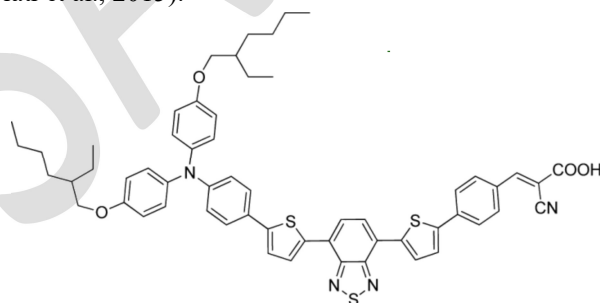

Fig. 53. Chemical structure of the target sensitizer (G3)

[Source: http://pubs.acs.org/doi/abs/10.1021/acssuschemeng.5b00108]

Accordingly, a sustainable approach was applied to a large extent from the initial stage of the molecular design of the dye (Agosta et al., 2014; Shibayama et al., 2014). This is because the implementation of further complex structures would have needed extra synthetic steps, inescapably leading to higher production of waste material and increased costs (Krebs & Jørgensen, 2013). For the very first time, a

comparison has been made between two synthetic protocols: a conventional approach that utilizes organo-metallic intermediates (used to validate the hypothesis on potentialities and efficacy of the dye) and secondly, an appropriately optimized course that is exclusively grounded on direct arylation reactions. The green metrics (yields on the whole, EcoScale parameter, E-factor) and the estimated price per gram of these two synthetic protocols have been calculated providing guiding principles that, if applied as good practice, will reduce the cost and the environmental impact associated with the production of the "green" technologies using organic materials (Po et al., 2014; 2015).
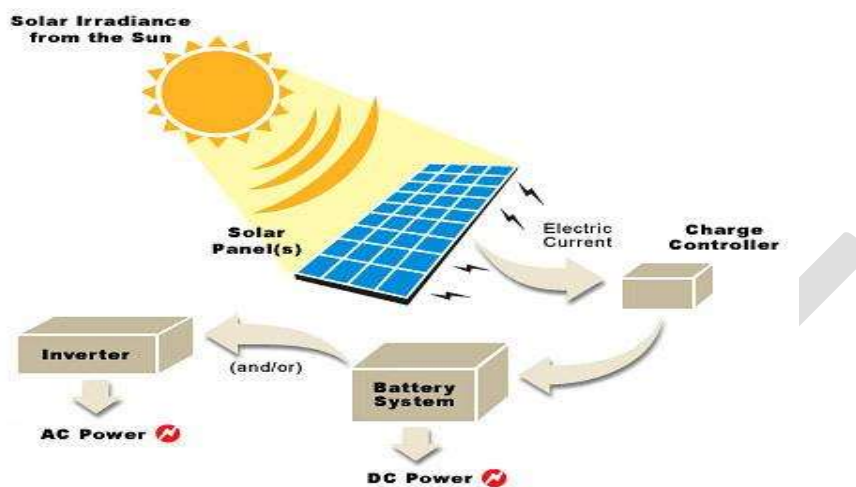

Fig. 54. Typical working principle of a solar cell

[Source: https://saferenvironment.wordpress.com/2009/02/02/solar-power-%E2%80%93-sustainable-green-energy-to-protect-our-economy-and-environment/]

While DSSCs carry on exhibiting expected competitive prices about those of the conventional silicon-based solar technologies, at the same time, the stability of the device is put at severe risk when organic sensitizers are employed as light-harvesters. The stability of ruthenium-based devices was anticipated to be around 25 years under Southern European ambient conditions using accelerated aging tests (Sheldon, 2007; 2010). As a result, once the environmental impact related to its costs and synthesis was evaluated, we deem it valuable to study the stability of the G3 sensitizer in an attractive DSSC application by employing transparent thin TiO_2 layers (Van Aken et al., 2006; Patel et al., 2012). In the case of cells containing G3, the drop in efficiency (15%) after 1000 h of aging at 85 °C of large area devices was observed to be extremely lower as compared to ruthenium-based devices.

2. Solar Cell Synthesis and Environmental Aspects

The plan of the first approach for the synthesis of G3 included using conventional Pd-catalyzed Suzuki cross-coupling steps (Route A), as explained in Scheme 1 (Kato et al., 2009; Harikisun & Desilvestro, 2011). The realization of the benzothiadiazole comprising of chromophore started from the commercially offered 4, 7-dibromo benzothiadiazole, which was delivered to a Suzuki cross-coupling

154

having thiophene-2-aryl boronic acid resulting in the corresponding diphenyl-derivative 1. The reaction between 1 and an equimolar quantity of N-bromosuccinimide (NBS) resulted in the corresponding promo-derivative 2; afterward, Bromo-derivative two was halogenated by reacting it with N-iodosuccinimide (NIS), which yielded compound 3. To bind together the electron group and the chromophore, a Suzuki coupling was carried out between 3 and the suitable triarylamine boronic ester β which led to the formation of intermediate 4, which, due to the halogen effect, is yet endowed with the bromide leaving the group. Following that, a Suzuki cross-coupling between 4-formyl-phenylboronic acid and 4 made it possible for us to acquire the aldehyde-functionalized precursor 5, which in the end, was converted into the target molecule G3 as a result of a Knoevenagel reaction with cyano-acetic acid.   After that, the acquired sensitizer was completely characterized via elemental analysis, NMR, UV−vis as well as by electro-spray ionization high-resolution mass spectrometry (ESI-HRMS) thatclearly confirmed its structure.
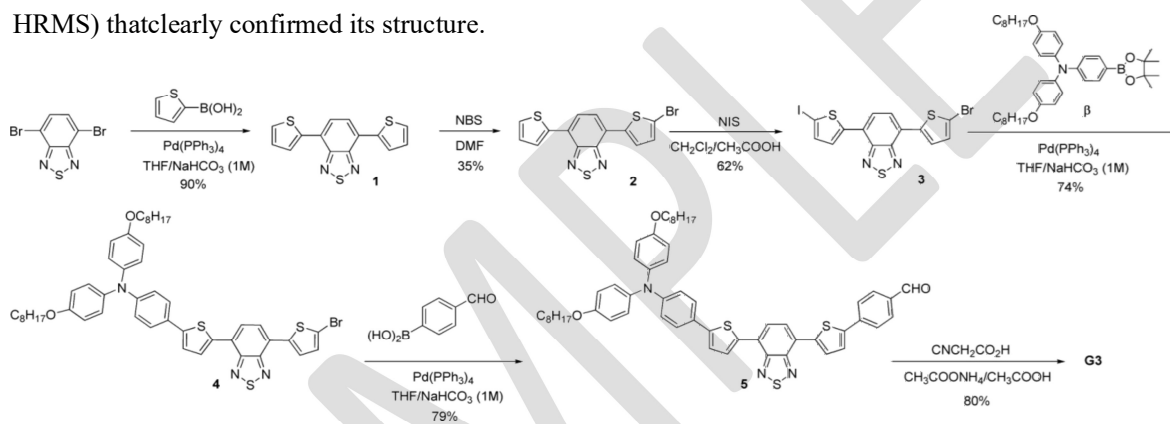

Fig. 55. Synthetic Sequence (Scheme-1) followed for obtaining G3 through a conventional Approach (Route A)

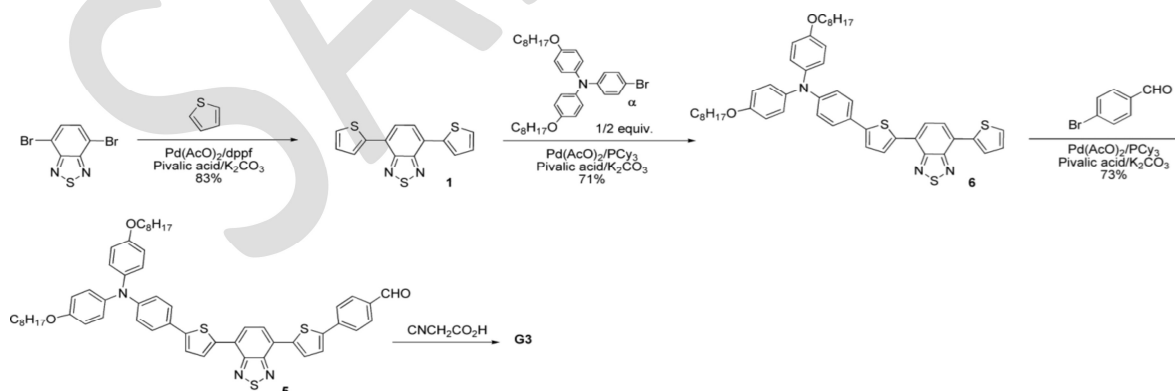[Source: http://pubs.acs.org/doi/abs/10.1021/acssuschemeng.5b00108]

Fig. 56. Synthetic Sequence (Scheme-2) followed for obtaining G3 through C−H Direct Arylations (Route B)

[Source: http://pubs.acs.org/doi/abs/10.1021/acssuschemeng.5b00108]

Subsequently, we felt motivated to investigate terms for a synthetic scale-up of the material, as well as exploring the environmental problems associated with its synthesis. Within this perspective, our investigation initiated by selecting E-factor, overall yields, and an EcoScale parameter related to the preparation of G3 to assess the sustainability of the first approach (Route A) from the waste generation, chemical, and safety point of view, respectively. Particularly, the high E-factor (15815.19 g/g) unable to get along with the large-scale production of the dye verified the requirement for sustainable and alternative approaches.

The simplest method for lessening the environmental effects of a chemical synthesis is reducing the total number of the synthetic steps. To pursue this goal for achieving G3, the most appropriate considered method is the setting up of a synthetic sequence based entirely on direct arylation reactions (Scheme 2) avoiding all metalation steps.

Sr. No.	Solvent	Ligand	Thiophene Equiv[a]	Yield (%)[B]
1	toluene	t-Bu$_3$P	1.0	traces
2	toluene	t-Bu$_3$P	5.0	8
3	toluene	t-Bu$_3$P	10.0	14
4	DMF	t-Bu$_3$P	10.0	traces
5	DMSO	t-Bu$_3$P	10.0	traces
6	thiophene	t-Bu$_3$P	20.8	35
7	thiophene	Cy$_3$P	20.8	38
8	thiophene	Ph$_3$P	20.8	47
9	thiophene	dppe	20.8	78
10	thiophene	dppf	20.8	83

Table 7. Tuning of the Reaction Conditions for obtaining 1 through Direct Arylation

a=per bromine atom; b=Isolated yields by crystallization or chromatography.

On this basis, we embarked in the unique synthesis of the chromophore 1 initiating from 4,7-dibromobenzothiadia-zole and triggering the C−H bonds on the thiophene by making use of Pd(AcO)2 as a source of palladium, pivalic acid (30% mol/ mol with regard to atoms of bromine) as a proton shuttle, K2CO3 (1.5 equiv. with regard to bromine atoms) as the base, and tri(t-butyl) phosphane (2.0 equiv. with regard to Pd) as the ligand (Cannavale et al., 2011; 2014; Matsidik et al., 2014; 2015). The preliminary screening of reaction conditions (as mentioned in Table 7) involved the relative amount of thiophene and the solvent. In the first attempts, to get better yields of the reaction, the impact of excess

thiophene (Sr. No. 1−3) was assessed in toluene as the solvent. Unluckily, under such conditions, the reaction was barely selective, most likely for the reason that after arylation of the initially activated 2-position of the thiophene unit, the thiophene 5-position of the formed intermediate turns into more reactive.

While we increase the polarity of the reaction medium (Table 7: No. 4 and 5), it did not improve the reaction selectivity. It is thus logical to presume that the acidity of the thiophene α-proton within thiophene-benzothiadiazole segment (and in its higher homologues) is stronger as compared to the acidity of the α-protons within isolated thiophene, owing to the existence of a strong electron withdrawing unit in the former (X. Wang, & M. Wang, 2014; Wang et al., 2015).

3.   ACS Sustainable Chemistry & Engineering

Apparently, thiophene is not much o prone toward the hydrogen abstraction step required for the direct arylation and is liable for the limited selectivity of the reaction under such conditions. On the other hand, if the reaction takes place within thiophene taken as the solvent (11.4 mL for each gram of dibromo benzothiadiazole, 20.8 equiv. for each bromine atom, No. 6), the yield of the reaction is increased to almost 35%. The strong, surplus thiophene reduced the side reactions by mass action, which led to an increase in the selectivity of the process, whereas the moderate yield appears to be connected with deactivation of the catalyst, which hindered a complete conversion of the substrate (Zhang et al., 2013; He et al., 2014). Consequently, the succeeding efforts made with an aim to improve the reaction course were directed at the exploration for a more robust catalytic system by conveniently varying the phosphine ligand. From the screening of the ligand (entries 6−10), it was obvious that aryl phosphanes are more performing as compared to aliphatic ones. In addition to this, apparently bidentate ligands (dppe and dppf) proved out to be the most suitable for this reaction. The reaction that was carried out in the company of dppf as the ligand permitted us to obtain 1 in 83% isolated yield.

Particular attention was given to the optimization of workup procedure to reduce the waste load derived from the reaction, i.e., the removal of the excess solvent (thiophene) was carried out by the distillation process. Additionally, the product was easily isolated by precipitation reaction involving a minimum quantity of ethanol/water mixture followed by formation of crystals from ethanol. The convenient isolation of the product was carried out due to the excellent solubility of K_2CO_3, pivalic acid and KBr byproducts. The purification step was facilitated by the nonexistence of organic byproducts resulting from side reactions. Interestingly, the excess thiophene was recovered by distillation followed by efficient recycling for further synthesis of 1 via activation of the C−H bond. The above mentioned purification process resulted in the attainment of the same parameters for purity and yield of the target compound, i.e., G3. The Calculation of the E-factor for this particular step of Route B (specifically the attainment of the building block 1) provided a value of 83.53 g/g, which is roughly one-sixth of the value, obtained for Route-A (478.57 g/g). The above practice represents a great progress regarding

waste creation for the attainment of the same product. In this framework, it is essential to note that the calculation of E-factor for the attainment of 1 in Route-A is undervalued. This is because of the reason that this calculation does not consider the use of formerly dried and distilled solvents (e.g., toluene, DMSO or DMF), which unavoidably leads to further production of waste. The above mentioned process provides an added value to the direct arylation process proposed in Route-B. The behavior of 1 under direct arylation was also investigated thoroughly to evaluate the environmental sustainability of asymmetric structure assemblies via subsequent activations of C−H bonds.

As illustrated in Scheme 2, binding of the donor-containing triarylamine group with benzothiadiazole-based chromophore takes place by the reaction of the bromo-derivative α with 1 using the standardized catalytic system of Pd(AcO)2/PCy3, to guarantee the attainment of soluble reaction products. The molar ratios (1/α) was varied to carry out the screening (Table 8). Differently from the other substrates containing two identical C−H activated positions thus far explored in direct monoarylations (thiophene or bithiophene), Unlike formerly investigated cases, the present case depicts that the utilization of 2.0 equivalent of 1 with reference to α is adequate to guarantee a satisfactory yield (i.e., 71% with reference to the limiting reactant). The results illustrated in Table 2 demonstrate that the reactivity of the C−H bonds in 1 is analogous with that in 6, due to the use of 1.0 equivalent of 1 concerning α (entry 1) which led to a virtual statistical distribution of products.

entry	equiv^a	recovered 1 (%)	monosub product (%)^c	disub product (%)^c
1	1.0	19	42	18
2	1.5	71^b	59	11
3	2.0	80^b	71	traces

^{a}Equiv of **1** with respect to **α**. ^{b}Calculated with respect to the used excess. ^{c}Isolated yields with respect to the limiting reactant (**α**).

Table 8. Product distribution of the reactions between α and 1 via Direct Arylation routes

4.   Comparison of Different Synthesis Approaches

The uses of 2.0 equivalent of 1 with reference to α make an appropriate compromise between yield minimization and maximization during the waste production originating from the utilization of excess reagents (the relative waste load associated with the synthesis of 1). These experimental conditions (particularly, the excess amounts of the powdery substance 1) do not impede the purification procedures. Amazingly, most of the one amount (80%) can be recovered, and only small amounts of the di-substituted product are formed. The utilization of a surplus of 1 leads to an increment in the E-factor during the reaction steps. It is well documented that the increase of E-factor improves the sustainability of the projected Route-B for large-scale potential applications. Moreover, the above procedure can also be employed for synthesis of a wide range of structures at laboratory scale. The path toward the fabrication of G3 via direct arylation procedures was further followed by improving the

reactive behavior of the asymmetric substance 6 in the 4-bromobenzaldehyde environment along with the presence of aldehyde precursor 5. It has been reported that the yield of the reaction involving the Pd (AcO) 2/PCy3 catalytic systems approaches 73%. The synthetic Route B has also been evaluated for calculation of green metrics for G3. The calculation results were compared with the ones obtained from the conventional method, i.e., Route A. It is obvious from the repeated results that the overall yield obtained with Route B is significantly higher than that obtained with Route A, representing the lesser number of synthetic steps. A preliminary deliberation has to be made regarding the environmental concerns associated with two different synthetic routes.

entry	Route A (traditional approach)	Route B (C−H activation)
overall yield (%)	1.7	10.7
E-factor (g/g)	15815.19	7706.91
EcoScale parameter	−161.2	−82.7
cost (€/g)	1117.14	505.45

Table 9. Cost Summary and Green Metric of the Two Processes for the attainment of the final sensitizer G3

The comparison of E-factor values attained for various approaches using a variety of raw materials must be made carefully. Usually, the projected step-by-step assembling of the target molecules in Route A does not follow the comparison step. On the other hand, commercially available, 4-formyl-phenylboronic acid and thiophene-2-aryl boronic acid necessitate further manufacturing steps to be synthesized. Route-A initiates the synthesis procedure by consuming the suitable raw materials (which are directly utilized as reactants in case of Route B); consequently, escalating the waste burden linked with Route A. At the same instance, in the case of activation reactions associated with C−H, an appropriate blend of chemicals has to be employed to create the catalytic system, which differs from the conventional Pd(PPh3)4 used in Suzuki cross couplings. Almost every commercial reactant possesses an environmental impact, which cannot be exploited by calculating the E-factor of the individual reaction steps.

It can be predicted that the cost analysis of a fine chemical substance can prove helpful for a comparative assessment of the environmental impacts linked to the chemical compound. This is because of the reason that the sale price of a chemical compound is also determined by the percentage of the waste burden present in the overall weight (Anderson, 2012; Butter et al., 2006). Considering the waste content of the chemical compounds, it is quite possible to obtain lower prices of the published catalogs by negotiation. However, the cost estimation of all intermediate compounds is established by the presently available prices of the raw materials. On the above mentioned basis, the projected per gram cost of G3 was evaluated for Route A (approx. 1117.14 €/g). The projected cost is enormously high for a fine chemical compound with prospective large-scale applications. On the contrary, the expected per

gram cost of G3 for Route B was approximately 505.45 €/g, exhibiting a huge improvement (Table 3). Although the higher costs do not directly influence the environment, the manufacturing choices resulting in a considerable cut-down in cost are essential in the view of achieving competitiveness to the solar cell technology (Osedach et al., 2013; Hendsbee et al., 2014). Immense benefits can also be obtained concerning waste production due to diminished E-factor calculation in Route B, i.e., 7706.91 g/g, which is half of the calculation obtained for Route-A. An additional key tool for the assessment of environmental impact of a process is the estimation of the Eco-Scale parameter. The evaluation of Eco-Scale parameter incorporates issues such as hazards and toxicity associated with the use of solvents, reagents, process setup, purification procedures, and prices. A higher value of Eco-Scale factor represents a better method. The values acquired for Route A and B. Low values are attained for Route-A and Route-B (−82.7 and −161.2 for Route B and A, respectively), due to the higher number of manufacturing steps. However, it is evident that Route B is exceptionally favorable concerning the traditional approach due to the presence of C−H activation pathway.

5.   Device Stability and Photovoltaic Properties

The photovoltaic potentials of G3 devices have been evaluated by developing a series of liquid electrolyte dye-sensitized solar cells. The power conversion efficiency of G3 (i.e., η = 8.64%) can be recognized as extraordinarily high. This is because power conversion efficiency of G3 is higher than that of the cells constructed from the ruthenium-based dye (N719) with the average lab-scale efficiency of around 8.3% (commonly recognized as a reference value in DSSCs). The higher conversion efficiencies of G3-based solar cells have motivated the scientists and researchers to explore this area of active devices.
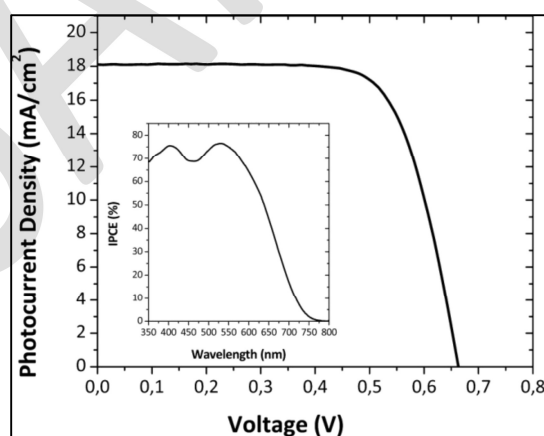

Fig. 57.   Relationship between photocurrent density and voltage (Curve of a G3-based solar cell device under 1.0 sun illumination (VOC = 0.663 V, JSC = 18.11 mA/cm2, FF = 0.72).

[Source: http://pubs.acs.org/doi/abs/10.1021/acssuschemeng.5b00108]

To evaluate the high efficiency of G3-based solar cells, the performances of transparent DSSC prototypes with a large-area have been investigated repeatedly before and after the aging test (at 85 °C for 1000 hours in variable ambient conditions) followed by the comparison of the results with the N719-based standard.

5.1. Effect of Aging Process

Before the aging process, short-circuit current (JSC) and open-circuit voltage (VOC) were analogous to both cells prepared by Grisorio et al. (2015). The values of JSC and VOC were independent of the used dye (N719 or G3). However, the N719-based solar cells exhibited a superior fill factor (FF) resulting in slightly higher increasing efficiencies (Fig.58A). The N719-based solar cell exhibited an efficiency drop of about 59% after undergoing aging for 1000 hours (Leonardi et al., 2010; Heo et al., 2013). On the other hand, the decrement in the efficiency of the G3 device was approximately 15% (Fig.58B).

Interpretation of the above data necessitates considering that the diffusion of water is only possible during a prolonged aging process in the dearth of any humidity control system at a constant aging temperature. The above-illustrated situation presents detailed information on the long-term stability of a particular dye.
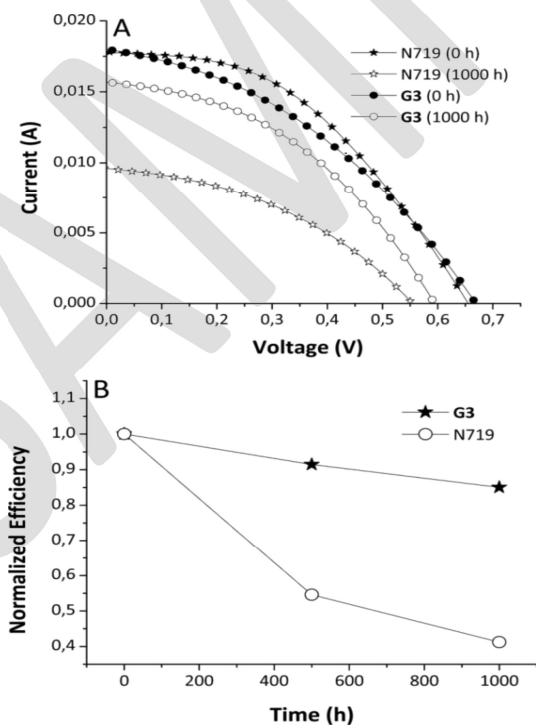

Fig. 58. (A) I−V characteristics for the two different dyes before and after aging at 85 °C for 1000 hours (potential scan direction was from high to low voltage). (B) Graph showing the relationship between efficiency decay and time during aging.

[Source: http://pubs.acs.org/doi/abs/10.1021/acssuschemeng.5b00108]

161

5.2. Effect of Aqueous Media on Electrochemical Properties the DSSCs

It can be stated that G3-based devices are comparatively less sensitive to aqueous media as compared to N719-based devices. This behavior can be illustrated by the trends in the values of circuit resistance tabulated in Table 10, acquired by electrochemical impedance spectroscopy (EIS, Fig.59).

Parameters	N719		G3	
Time (hours)	0	0	1000	1000
Rrec (ohm)	1.72	0.71	0.59	1.34
Rct (ohm × cm^2)	8.77	9.53	9.60	14.06
Rd (ohm)	2.24	2.05	2.55	3.82

Table 10. Fitting Data from EIS Plots

Rct: charge transfer resistance at the Platinum layer. Rd: diffusion resistance of the redox pair in the electrolyte. Rrec: recombination resistance at the dye / TiO$_2$−electrolyte interface

The values given in Table 10 are stringently associated with each other and their deviation with time is considered to be dependent on three major reasons which are listed below.

  i.   Electrolyte bleaching (lessening the concentration of I$_3^-$ in the electrolyte)

  ii.   Decrease in catalytic activity of Pt-based counter-electrode

  iii. Detachment of the dye from the TiO$_2$ surface

The decrease in the recombination resistance (Rrec) suggests an increment in the recombination rate of the injected mobile electrons onto the surface of TiO2. The mobile electrons instigate the presence of the oxidized state of the redox couple in the electrolyte system due to dye detachment from the photoanode (Heo et al., 2013). It can be logically assumed that the above mentioned drawback is caused due to the hydrolysis reaction in the presence of the titanium carboxylate bonding between TiO2 and the dye surface, triggered by the traces of water (Li et al., 2014; 2015). On the other hand, a sharp decrement in Rrec and Isc is observed for N719. This observation can be associated with two distinct effects caused by the interaction of water with the dye and TiO2, i.e., dye modification and dye detachment from the surface of TiO2 (Nguyen et al., 2007; 2009; 2010).

To further validate the water effect, the increment in the diffusion resistance (Rd) in both cases was observed after the aging process ((Papageorgiou et al., 1997; Nour-Mohammadi et al., 2007). This increment can be caused due to the bleaching of the electrolyte with time, as already illustrated in the literature (Hauch & Georg, 2001; Asghar et al., 2012; Mastroianni et al., 2014). Bleaching of the

electrolyte can be caused by the formation of iodate in the aqueous medium (Macht et al., 2002; Jung et al., 2009; Modestino & Haussener, 2015).
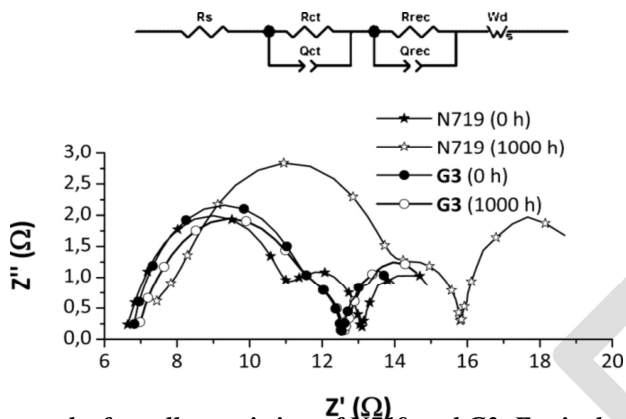

Fig. 59. Nyquist graphs for cells consisting of N719 and G3. Equivalent circuit employed for curve fitting of the impedance data: Rct/Qct charge transfer, capacitance and Rs series resistance at the surface of platinum (semicircle at high frequency); Capacitance and Rrec/Qrec recombination resistance at the dye/titania-electrolyte interface (i.e., semicircle at intermediate frequency); Semicircle at low frequency represents Wd diffusion

[Source: http://pubs.acs.org/doi/abs/10.1021/acssuschemeng.5b00108]

References

[1] Zhang, S., Yang, X., Numata, Y., & Han, L. (2013). Highly efficient dye-sensitized solar cells: progress and future challenges. *Energy & Environmental Science*, *6*(5), 1443-1464.

[2] Liang, M., & Chen, J. (2013). Arylamine organic dyes for dye-sensitized solar cells. *Chemical Society Reviews*, *42*(8), 3453-3488.

[3] Yen, Y. S., Chou, H. H., Chen, Y. C., Hsu, C. Y., & Lin, J. T. (2012). Recent developments in molecule-based organic materials for dye-sensitized solar cells. *Journal of Materials Chemistry*, *22*(18), 8734-8747.

[4] Ooyama, Y., Nagano, T., Inoue, S., Imae, I., Komaguchi, K., Ohshita, J., & Harima, Y. (2011). Dye-Sensitized Solar Cells Based on Donor-π-Acceptor Fluorescent Dyes with a Pyridine Ring as an Electron-Withdrawing-Injecting Anchoring Group. *Chemistry-A European Journal*, *17*(52), 14837-14843.

[5] Ooyama, Y., & Harima, Y. (2012). Photophysical and Electrochemical Properties, and Molecular Structures of Organic Dyes for Dye-Sensitized Solar Cells. *ChemPhysChem*, *13*(18), 4032-4080.

[6] Ooyama, Y., & Harima, Y. (2013). Corrigendum: Photophysical and Electrochemical Properties, and Molecular Structures of Organic Dyes for Dye-Sensitized Solar Cells. *ChemPhysChem*, *14*(5), 871-871.

[7] Mishra, A., Fischer, M. K., & Bäuerle, P. (2009). Metal-free organic dyes for dye-sensitized solar cells: From structure: Property relationships to design rules. *Angewandte Chemie International Edition*, *48*(14), 2474-2499.

[8] O'regan, B., & Grätzel, M. (1991). A low-cost, high-efficiency solar cell based on dye-sensitized colloidal TiO 2 films. *nature*, *353*(6346), 737-740.

[9] Zeng, W., Cao, Y., Bai, Y., Wang, Y., Shi, Y., Zhang, M., & Wang, P. (2010). Efficient dye-sensitized solar cells with an organic photosensitizer featuring orderly conjugated ethylenedioxythiophene and dithienosilole blocks. *Chemistry of Materials*, *22*(5), 1915-1925.

[10] Yum, J. H., Baranoff, E., Wenger, S., Nazeeruddin, M. K., & Grätzel, M. (2011). Panchromatic engineering for dye-sensitized solar cells. *Energy & Environmental Science*, *4*(3), 842-857.

[11] Ogura, R. Y., Nakane, S., Morooka, M., Orihashi, M., Suzuki, Y., & Noda, K. (2009). High-performance dye-sensitized solar cell with a multiple dye system. *Applied Physics Letters*, *94*(7), 54.

[12] Fan, S. Q., Kim, C., Fang, B., Liao, K. X., Yang, G. J., Li, C. J., & Ko, J. (2011). Improved efficiency of over 10% in dye-sensitized solar cells with a ruthenium complex and an organic dye

heterogeneously positioning on a single TiO2 electrode. *The Journal of Physical Chemistry C*, *115*(15), 7747-7754.

[13]   Fakharuddin, A., Jose, R., Brown, T. M., Fabregat-Santiago, F., & Bisquert, J. (2014). A perspective on the production of dye-sensitized solar modules. *Energy & Environmental Science*, *7*(12), 3952-3981.

[14]   Zardetto, V., Di Giacomo, F., Garcia-Alonso, D., Keuning, W., Creatore, M., Mazzuca, C., & Brown, T. M. (2013). Fully Plastic Dye Solar Cell Devices by Low-Temperature UV-Irradiation of both the Mesoporous TiO2 Photo-and Platinized Counter-Electrodes. *Advanced Energy Materials*, *3*(10), 1292-1298.

[15]   Matteocci, F., Cinà, L., Di Giacomo, F., Razza, S., Palma, A. L., Guidobaldi, A., & Di Carlo, A. (2016). High efficiency photovoltaic module based on mesoscopic organometal halide perovskite. *Progress in Photovoltaics: Research and Applications*, *24*(4), 436-445.

[16]   Hagfeldt, A., Boschloo, G., Sun, L., Kloo, L., & Pettersson, H. (2010). Dye-sensitized solar cells. *Chemical reviews*, *110*(11), 6595-6663.

[17]   Yella, A., Lee, H. W., Tsao, H. N., Yi, C., Chandiran, A. K., Nazeeruddin, M. K., ... & Grätzel, M. (2011). Porphyrin-sensitized solar cells with cobalt (II/III)–based redox electrolyte exceed 12 percent efficiency. *science*, *334*(6056), 629-634.

[18]   Mishra, A., Fischer, M. K., & Bäuerle, P. (2009). Metal-free organic dyes for dye-sensitized solar cells: From structure: Property relationships to design rules. *Angewandte Chemie International Edition*, *48*(14), 2474-2499.

[19]   Gao, P., Grätzel, M., & Nazeeruddin, M. K. (2014). Organohalide lead perovskites for photovoltaic applications. *Energy & Environmental Science*, *7*(8), 2448-2463.

[20]   Sum, T. C., & Mathews, N. (2014). Advancements in perovskite solar cells: photophysics behind the photovoltaics. *Energy & Environmental Science*, *7*(8), 2518-2534.

[21]   Green, M. A., Ho-Baillie, A., & Snaith, H. J. (2014). The emergence of perovskite solar cells. *Nature Photonics*, *8*(7), 506-514.

[22]   Wu, Y., & Zhu, W. (2013). Organic sensitizers from D–π–A to D–A–π–A: effect of the internal electron-withdrawing units on molecular absorption, energy levels and photovoltaic performances. *Chemical Society Reviews*, *42*(5), 2039-2058.

[23]   Wu, Y., Marszalek, M., Zakeeruddin, S. M., Zhang, Q., Tian, H., Grätzel, M., & Zhu, W. (2012). High-conversion-efficiency organic dye-sensitized solar cells: molecular engineering on D–A–π-A featured organic indoline dyes. *Energy & Environmental Science*, *5*(8), 8261-8272.

[24]   Yen, Y. S., Chou, H. H., Chen, Y. C., Hsu, C. Y., & Lin, J. T. (2012). Recent developments in molecule-based organic materials for dye-sensitized solar cells. *Journal of Materials Chemistry*, *22*(18), 8734-8747.

[25]   Burke, D. J., & Lipomi, D. J. (2013). Green chemistry for organic solar cells. *Energy & Environmental Science*, *6*(7), 2053-2066.

[26]   Osedach, T. P., Andrew, T. L., & Bulović, V. (2013). Effect of synthetic accessibility on the commercial viability of organic photovoltaics. *Energy & Environmental Science*, *6*(3), 711-718.

[27]   Po, R., Bernardi, A., Calabrese, A., Carbonera, C., Corso, G., & Pellegrino, A. (2014). From lab to fab: how must the polymer solar cell materials design change?–an industrial perspective. *Energy & Environmental Science*, *7*(3), 925-943.

[28]   He, C. Y., Wu, C. Z., Zhu, Y. L., & Zhang, X. (2014). Selective thienylation of fluorinated benzothiadiazoles and benzotriazoles for organic photovoltaics. *Chemical Science*, *5*(4), 1317-1321.

[29]   Xiao, Y. L., Zhang, B., He, C. Y., & Zhang, X. (2014). Direct Olefination of Fluorinated Benzothiadiazoles: A New Entry to Optoelectronic Materials. *Chemistry-A European Journal*, *20*(16), 4532-4536.

[30]   Xing, H., Chen, L., Jia, Y., Jiang, Z., & Yang, Z. (2017). Fe 2 O 3-catalyzed Pummerer rearrangement of acyl chlorides and sulfoxides: Facile synthesis of alkylthiomethyl ester. *Tetrahedron Letters*, *58*(23), 2199-2202.

[31]   Zhang, J., Chen, W., Rojas, A. J., Jucov, E. V., Timofeeva, T. V., Parker, T. C., & Marder, S. R. (2013). Controllable direct arylation: Fast route to symmetrical and unsymmetrical 4, 7-diaryl-5, 6-difluoro-2, 1, 3-benzothiadiazole derivatives for organic optoelectronic materials. *Journal of the American Chemical Society*, *135*(44), 16376-16379.

[32]   He, C. Y., Wu, C. Z., Qing, F. L., & Zhang, X. (2014). Direct (Het) arylation of fluorinated benzothiadiazoles and benzotriazole with (Het) aryl iodides. *The Journal of organic chemistry*, *79*(4), 1712-1718.

[33]   Zhang, J., Kang, D. Y., Barlow, S., & Marder, S. R. (2012). Transition metal-catalyzed C–H activation as a route to structurally diverse di (arylthiophenyl)-diketopyrrolopyrroles. *Journal of Materials Chemistry*, *22*(40), 21392-21394.

[34]   Schipper, D. J., & Fagnou, K. (2011). Direct arylation as a synthetic tool for the synthesis of thiophene-based organic electronic materials. *Chemistry of Materials*, *23*(6), 1594-1600.

[35]   Mercier, L. G., & Leclerc, M. (2013). Direct (hetero) arylation: a new tool for polymer chemists. *Accounts of chemical research*, *46*(7), 1597-1605.

[36]   Berrouard, P., Najari, A., Pron, A., Gendron, D., Morin, P. O., Pouliot, J. R., & Leclerc, M. (2012). Synthesis of 5-Alkyl [3, 4-c] thienopyrrole-4, 6-dione-Based Polymers by Direct Heteroarylation. *Angewandte Chemie International Edition*, *51*(9), 2068-2071.

[37]   Kang, X., Zhang, J., O'Neil, D., Rojas, A. J., Chen, W., Szymanski, P., & El-Sayed, M. A. (2014). Effect of molecular structure perturbations on the performance of the D–A− π–A dye sensitized solar cells. *Chemistry of Materials*, *26*(15), 4486-4493.

[38]   Joly, D., Pelleja, L., Narbey, S., Oswald, F., Meyer, T., Kervella, Y., & Demadrille, R. (2015). Metal-free organic sensitizers with narrow absorption in the visible for solar cells exceeding 10% efficiency. *Energy & Environmental Science*, *8*(7), 2010-2018.

[39]   Chai, Q., Li, W., Liu, J., Geng, Z., Tian, H., & Zhu, W. H. (2015). Rational molecular engineering of cyclopentadithiophene-bridged DA-π-A sensitizers combining high photovoltaic efficiency with rapid dye adsorption. *Scientific reports*, *5*, srep11330.

[40]   Kang, X., Zhang, J., Rojas, A. J., O'Neil, D., Szymanski, P., Marder, S. R., & El-Sayed, M. A. (2014). Deposition of loosely bound organic D–A–π–A′ dyes on sensitized TiO 2 film: a possible strategy to suppress charge recombination and enhance power conversion efficiency in dye-sensitized solar cells. *Journal of Materials Chemistry A*, *2*(29), 11229-11234.

[41]   Li, H., Wu, Y., Geng, Z., Liu, J., Xu, D., & Zhu, W. (2014). Co-sensitization of benzoxadiazole based D–A–π–A featured sensitizers: compensating light-harvesting and retarding charge recombination. *Journal of Materials Chemistry A*, *2*(35), 14649-14657.

[42]   Echeverry, C. A., Cotta, R., Castro, E., Ortiz, A., Echegoyen, L., & Insuasty, B. (2015). New organic dyes with high IPCE values containing two triphenylamine units as co-donors for efficient dye-sensitized solar cells. *RSC Advances*, *5*(75), 60823-60830.

[43]   Jiang, S., Fan, S., Lu, X., Zhou, G., & Wang, Z. S. (2014). Double D–π–A branched organic dye isomers for dye-sensitized solar cells. *Journal of Materials Chemistry A*, *2*(40), 17153-17164.

[44]   Double, D. (2014). π-A branched organic dye isomers for dye-sensitized solar cells Jiang, Shenghui; Fan, Suhua; Lu, Xuefeng; Zhou, Gang; Wang, Zhong-Sheng. *Journal of Materials Chemistry A: Materials for Energy and Sustainability*, *2*(40), 17153-17164.

[45]   Feng, Q., Zhang, Q., Lu, X., Wang, H., Zhou, G., & Wang, Z. S. (2013). Facile and selective synthesis of oligothiophene-based sensitizer isomers: an approach toward efficient dye-sensitized solar cells. *ACS applied materials & interfaces*, *5*(18), 8982-8990.

[46]   Qian, X., Gao, H. H., Zhu, Y. Z., Lu, L., & Zheng, J. Y. (2015). Biindole-based double D–π–A branched organic dyes for efficient dye-sensitized solar cells. *RSC Advances*, *5*(6), 4368-4375.

[47]   Qian, X., Gao, H. H., Zhu, Y. Z., Pan, B., & Zheng, J. Y. (2015). Tetraindole-based saddle-shaped organic dyes for efficient dye-sensitized solar cells. *Dyes and Pigments*, *121*, 152-158.

[48]   Grisorio, R., De Marco, L., Agosta, R., Iacobellis, R., Giannuzzi, R., Manca, M., & Suranna, G. P. (2014). Enhancing Dye-Sensitized Solar Cell Performances by Molecular Engineering: Highly Efficient π-Extended Organic Sensitizers. *ChemSusChem*, *7*(9), 2659-2669.

[49]   Roiati, V., Giannuzzi, R., Lerario, G., Marco, L. D., Agosta, R., Iacobellis, R., & Gigli, G. (2015). Beneficial Role of a Bulky Donor Moiety in π-Extended Organic Dyes for Mesoscopic TiO2 Sensitized Solar Cells. *The Journal of Physical Chemistry C*, *119*(13), 6956-6965.

[50]   Liu, D. S., Ding, W. L., Zhu, K. L., Geng, Z. Y., Wang, D. M., & Zhao, X. L. (2014). The master factors influencing the efficiency of D–A–π–A configured organic sensitizers in dye-sensitized solar cell via theoretically characterization: design and verification. *Dyes and Pigments*, *105*, 192-201.

[51]   Agosta, R., Grisorio, R., De Marco, L., Romanazzi, G., Suranna, G. P., Gigli, G., & Manca, M. (2014). An engineered co-sensitization system for highly efficient dye solar cells. *Chemical Communications*, *50*(67), 9451-9453.

[52]   Shibayama, N., Ozawa, H., Abe, M., Ooyama, Y., & Arakawa, H. (2014). A new cosensitization method using the Lewis acid sites of a TiO 2 photoelectrode for dye-sensitized solar cells. *Chemical Communications*, *50*(48), 6398-6401.

[53]   Krebs, F. C., & Jørgensen, M. (2013). Polymer and organic solar cells viewed as thin film technologies: What it will take for them to become a success outside academia. *Solar Energy Materials and Solar Cells*, *119*, 73-76.

[54]   Po, R., Bianchi, G., Carbonera, C., & Pellegrino, A. (2015). "All That Glisters Is Not Gold": an analysis of the synthetic complexity of efficient polymer donors for polymer solar cells. *Macromolecules*, *48*(3), 453-461.

[55]   Po, R., Bernardi, A., Calabrese, A., Carbonera, C., Corso, G., & Pellegrino, A. (2014). From lab to fab: how must the polymer solar cell materials design change?–an industrial perspective. *Energy & Environmental Science*, *7*(3), 925-943.

[56]   Sheldon, R. A. (2007). The E factor: fifteen years on. *Green Chemistry*, *9*(12), 1273-1283.

[57]   Sheldon, R. (2010). Introduction to green chemistry, organic synthesis and pharmaceuticals. *Green chemistry in the pharmaceutical industry*, 1-20.

[58]   Van Aken, K., Strekowski, L., & Patiny, L. (2006). EcoScale, a semi-quantitative tool to select an organic preparation based on economic and ecological parameters. *Beilstein journal of organic chemistry*, *2*(1), 3.

[59]   Patel, P. V., Joshi, N., & Panchal, D. P. (2012). Process for preparation of 5-(2-ethoxy-5-((4-methylpiperazin-1-yl) sulfonyl) phenyl)-3-isobutyl-1-methyl-1H-pyrazolo [4, 3-d] pyrimidin-7 (6H)-one (sildenafil citrate impurity). *Indian Patent Application No. IN 2012MU02516 A*, *20140606*, 29.

[60]   Harikisun, R., & Desilvestro, H. (2011). Long-term stability of dye solar cells. *Solar Energy*, *85*(6), 1179-1188.

[61]   Kato, N., Takeda, Y., Higuchi, K., Takeichi, A., Sudo, E., Tanaka, H., & Toyoda, T. (2009). Degradation analysis of dye-sensitized solar cell module after long-term stability test under outdoor working condition. *Solar Energy Materials and Solar Cells*, *93*(6), 893-897.

[62]   Cannavale, A., Manca, M., De Marco, L., Grisorio, R., Carallo, S., Suranna, G. P., & Gigli, G. (2014). Photovoltachromic device with a micropatterned bifunctional counter electrode. *ACS applied materials & interfaces*, *6*(4), 2415-2422.

[63]   Cannavale, A., Manca, M., Malara, F., De Marco, L., Cingolani, R., & Gigli, G. (2011). Highly efficient smart photovoltachromic devices with tailored electrolyte composition. *Energy & Environmental Science*, *4*(7), 2567-2574.

[64]   Matsidik, R., Martin, J., Schmidt, S., Obermayer, J., Lombeck, F., Nübling, F., & Sommer, M. (2014). C–H Arylation of Unsubstituted Furan and Thiophene with Acceptor Bromides: Access to Donor–Acceptor–Donor-Type Building Blocks for Organic Electronics. *The Journal of organic chemistry*, *80*(2), 980-987.

[65]   Matsidik, R., Komber, H., & Sommer, M. (2015). Rational Use of Aromatic Solvents for Direct Arylation Polycondensation: C–H Reactivity versus Solvent Quality. *ACS Macro Letters*, *4*(12), 1346-1350.

[66]   Wang, X., Wang, K., & Wang, M. (2015). Synthesis of conjugated polymers via an exclusive direct-arylation coupling reaction: a facile and straightforward way to synthesize thiophene-flanked benzothiadiazole derivatives and their copolymers. *Polymer Chemistry*, *6*(10), 1846-1855.

[67]   Wang, X., & Wang, M. (2014). Synthesis of donor–acceptor conjugated polymers based on benzo [1, 2-b: 4, 5-b′] dithiophene and 2, 1, 3-benzothiadiazole via direct arylation polycondensation: towards efficient C–H activation in nonpolar solvents. *Polymer Chemistry*, *5*(19), 5784-5792.

[68]   He, C. Y., Wu, C. Z., Qing, F. L., & Zhang, X. (2014). Direct (Het) arylation of fluorinated benzothiadiazoles and benzotriazole with (Het) aryl iodides. *The Journal of organic chemistry*, *79*(4), 1712-1718.

[69]   Zhang, J., Chen, W., Rojas, A. J., Jucov, E. V., Timofeeva, T. V., Parker, T. C., ... & Marder, S. R. (2013). Controllable direct arylation: Fast route to symmetrical and unsymmetrical 4, 7-diaryl-5, 6-difluoro-2, 1, 3-benzothiadiazole derivatives for organic optoelectronic materials. *Journal of the American Chemical Society*, *135*(44), 16376-16379.

[70]   Anderson, N. G. (2012). *Practical process research and development: a guide for organic chemists*. Academic Press.

[71]   Butters, M., Catterick, D., Craig, A., Curzons, A., Dale, D., Gillmore, A., & White, W. (2006). Critical Assessment of Pharmaceutical Processes A Rationale for Changing the Synthetic Route. *Chemical reviews*, *106*(7), 3002-3027.

[72]   Osedach, T. P., Andrew, T. L., & Bulović, V. (2013). Effect of synthetic accessibility on the commercial viability of organic photovoltaics. *Energy & Environmental Science*, *6*(3), 711-718.

[73]   Hendsbee, A. D., Macaulay, C. M., & Welch, G. C. (2014). Synthesis of an H-aggregated thiophene–phthalimide based small molecule via microwave assisted direct arylation coupling reactions. *Dyes and Pigments*, *102*, 204-209.

[74]   Heo, N., Jun, Y., & Park, J. H. (2013). Dye molecules in electrolytes: new approach for suppression of dye-desorption in dye-sensitized solar cells. *Scientific reports*, *3*.

[75]   Leonardi, E., Penna, S., Brown, T. M., Di Carlo, A., & Reale, A. (2010). Stability of dye-sensitized solar cells under light soaking test. *Journal of Non-Crystalline Solids*, *356*(37), 2049-2052.

[76]   Nguyen, P. T., Andersen, A. R., Skou, E. M., & Lund, T. (2010). Dye stability and performances of dye-sensitized solar cells with different nitrogen additives at elevated temperatures—Can sterically hindered pyridines prevent dye degradation?. *Solar Energy Materials and Solar Cells*, *94*(10), 1582-1590.

[77]   Nguyen, P. T., Degn, R., Nguyen, H. T., & Lund, T. (2009). Thiocyanate ligand substitution kinetics of the solar cell dye Z-907 by 3-methoxypropionitrile and 4-tert-butylpyridine at elevated temperatures. *Solar Energy Materials and Solar Cells*, *93*(11), 1939-1945.

[78]   Nguyen, H. T., Ta, H. M., & Lund, T. (2007). Thermal thiocyanate ligand substitution kinetics of the solar cell dye N719 by acetonitrile, 3-methoxypropionitrile, and 4-tert-butylpyridine. *Solar Energy Materials and Solar Cells*, *91*(20), 1934-1942.

[79]   Nour-Mohammadi, F., Nguyen, H. T., Boschloo, G., & Lund, T. (2007). An investigation of the photosubstitution reaction between N719-dyed nanocrystalline TiO 2 particles and 4-tert-butylpyridine. *Journal of Photochemistry and Photobiology A: Chemistry*, *187*(2), 348-355.